Non-destructive quantitation of spermine in human prostate tissue samples using HRMAS ¹H NMR spectroscopy at 9.4 T

Leo Ling Cheng[a],*, Chin-lee Wu[a], Matthew R. Smith[b], R. Gilberto Gonzalez[c]

[a]*Department of Pathology, Massachusetts General Hospital, Harvard Medical School, Boston, MA 02114, USA*
[b]*Department of Hematology and Oncology, Massachusetts General Hospital, Harvard Medical School, Boston, MA 02114, USA*
[c]*Department of Radiology, Massachusetts General Hospital, Harvard Medical School, Boston, MA 02114, USA*

Abstract We present the results of a study of human prostate specimens evaluated by high resolution magic angle spinning ¹H nuclear magnetic resonance (NMR) spectroscopy at 400 MHz (9.4 T) and by quantitative histopathology. We demonstrate that NMR and pathology data can be obtained from the same intact specimens, and report for the first time a linear correlation between the NMR measured concentration of spermine, a proposed endogenous inhibitor to prostate cancer growth, and the volume percentage of normal prostatic epithelial cells as quantified by histopathology. Our results show that NMR may serve as a critical tool for the investigation of the inhibitory mechanism of spermine in human subjects. © 2001 Published by Elsevier Science B.V. on behalf of the Federation of European Biochemical Societies.

Key words: Human prostate; Spermine; Proton nuclear magnetic resonance spectroscopy; High resolution magic angle spinning; Intact tissue specimen; Citrate

1. Introduction

The controversy surrounding prostate cancer has presented great challenges to medical and scientific communities and has generated enormous concerns in the public. The dilemma is highlighted by the increasingly high incidence of diagnoses resulting from improved detecting technologies, the relatively moderate mortality rate of many prostate cancer cases, and the high probability of complications accompanying local treatments. Clinical data indicate that compared with other malignancies, primary prostate cancers grow at a relatively slow rate, but the growth rates of prostate cancer at distant metastatic sites are similar to other more aggressive malignancies.

The seemingly indolent characteristic of organ-confined prostate cancer has been a focus of studies seeking to understand the inhibitory mechanism and to exploit its potential utility in therapy regimens [1–3]. As one such inhibitor, sper-

mine has shown down-regulatory effects on the growth of prostate cancer cells when analyzed in vitro, and has thus generated a number of intriguing questions with respect to its function in human prostate [1]. Direct answers to these questions can only be obtained from studies of human subjects; however, the use of human specimens presents a number of vexing challenges not faced by studies of cell lines.

Chief among these challenges are the so called 'sampling errors' raised from heterogeneity of cancer tissues. By any rigorous standard, very little may confidently be assumed regarding the biology and biochemistry of a particular region in an individual tumor, unless specimens from that tumor region are evaluated directly. This requirement, however, often poses a serious incompatibility between the procedures of histopathology and biochemistry. Thus, any study that investigates correlations between biochemistry and pathology, the 'gold standard' for cancer diagnosis, must make use of bio-analytical procedures that are non-destructive and transparent to histopathological evaluation.

Nuclear magnetic resonance (NMR) spectroscopy, a non-invasive technique, has been considered as a promising candidate to accomplish this task [4]. Intact specimens and extract solutions of tissue from prostate cancer patients have been studied by using conventional solution proton NMR methods [5–8]. However, because solution methods are not optimized for intact tissue analysis, and because the destructive procedures of the tissue extraction prevent further histopathological evaluation, correlations between NMR results and pathology have proven to be difficult to reach.

Here, we address this obstacle by using high resolution magic angle spinning (HRMAS), a NMR methodology developed for the analysis of intact tissue specimens [9,10]. HRMAS significantly differs from solution methods used in previous studies [5,8]. Specifically, HRMAS allows us to obtain high resolution spectra from intact tissue, comparable to those achievable with aqueous extract solutions, but preserves the tissue structures necessary for subsequent histopathological examinations.

Our results show, for the first time, that spermine in human prostate quantified by NMR correlates with the volume percentage (vol%) of normal prostatic epithelial cells measured by histopathology. The connection between spermine and prostate pathology, as the first step towards the investigation of the mechanism of spermine on prostate cancer growth, suggests that the hypothesized inhibitory function of spermine can now be clinically examined through NMR studies of human subjects.

---

*Corresponding author. Pathology Research CNY-7, 149 13th street, Charlestown, MA 02129, USA. Fax: (1)-617-726 5684.
E-mail: cheng@nmr.mgh.harvard.edu

2. Materials and methods

Use of human materials in the study was reviewed and approved by the IRB at the Massachusetts General Hospital, Boston, MA, USA.

2.1. Tissue specimens

Human prostate specimens used for this study ($n = 16$) were obtained from the tissue repository at the Cancer Center of the Massachusetts General Hospital. Patients' medical records showed that among these cases, nine were adenocarcinomas having a Gleason score of 6/10 (grades: 3/5+3/5, age 60.5 ± 1.7), six had a score of 7/10 (grades: 3/5+4/5, age 63.8 ± 2.1), and one was a surgical specimen collected as a normal control for research. No therapy was administered to the cancer patients prior to the surgery.

Tissue specimens were snap-frozen in liquid nitrogen and maintained at −80°C until the time of spectroscopic analysis. Approximately 50–100 mg of tissue from each case was obtained. Each specimen was divided into two halves. One half was used for the NMR analysis; the other half was saved for histopathological evaluation in order to determine the histopathological integrity of the specimen after NMR analysis. Before NMR analysis, frozen specimens were cut and weighed (between 16.3 and 47.0 mg, mean 35.7 ± 2.2 mg), positioned within a HRMAS rotor, and transferred into the NMR probe-head pre-cooled to 3°C. The NMR study, performed at 3°C, began immediately at tissue thawing. Directly after the NMR study, the specimens were fixed for subsequent quantitative histopathology examinations.

2.2. Quantitative histopathology

Tissue samples were fixed in 10% formalin, embedded in paraffin, cut into 5-micron sections, and stained with hematoxylin and eosin. Specimens that were obtained from 15 cases of clinically proven prostate cancer and that were measured with NMR were subjected to serial sections of one slide per 50–60 microns, while only one random slide was sectioned from the other half of a specimen that was not studied by NMR. Serial sections yielded 10–24 histopathological slides depending on the size and orientation of the individual sample.

Cross-sections of each sample were quantified by a microscopic image analyzer Image-Pro PLUS™ (Media Cybernetics®, Silver Spring, MD, USA). The percentages of areas representing cancer cells, normal epithelial cells and stroma structures in each cross-section were estimated visually to the nearest 5% by a single pathologist who did not have knowledge of the spectroscopic results. The reported vol% of each pathological presentation was calculated based on the size of the cross-section and the corresponding area percentages of each pathological feature. All slides were evaluated twice in a random order by the same pathologist over a time interval of 10 months. The data from these two evaluations were averaged to calculate vol%.

2.3. Proton NMR spectroscopy

The procedures used for NMR measurements and data processing have previously been described [10]. In brief, the HRMAS experiments were performed at 3°C on an MSL400 NMR spectrometer (proton frequency at 400.13 MHz) by using a BD-MAS probe; temperature was controlled by a VT-1000 unit, in combination with a MAS-DB pneumatic unit (Bruker Instruments, Inc., Billerica, MA, USA). Sample spinning rates were in the range of 2.34–2.49 kHz (± 2 Hz). A rotor-synchronized Carr–Purcell–Meibom–Gill (CPMG) pulse sequence (90-(τ-180-τ)$_n$ acquisition) was used to function as a T2 filter to suppress broad signals from macromolecules. The inter-pulse delay ($\tau = 2\pi/\omega_r$) was synchronized with the rotor rotation (τ indicates the sample spinning rate in time units and $\omega_r/2\pi$ represents the spinning rate in kHz). The value of n for each sample was adjusted to create a T2 filter of $2n\tau = 50$ ms. The 90° pulse length, which varied from 8.6 to 10.9 μs, was also adjusted individually for each sample. The number of transients was 256, with an acquisition time of 10 ms. A repetition time of 5.0 s, a spectral width of 8 kHz (20 ppm), and 16 time domain data points were employed. Spectra were collected both with and without suppression of resonance signals from tissue water. Water presaturation was achieved with a DANTE type pulse sequence (θ–τ)$_n$, where $\theta = 2.5$ μs and $n = 2000$, placed prior to the CPMG pulse sequence.

Spectroscopic data were processed with NMR1 software (New Method Research, Inc., Syracuse, NY, USA). All free induction de-

cays were subjected to 1 Hz apodization before Fourier transformation and phase adjustment. Regional integrals of the cellular metabolites from 0.5 to 4.5 ppm in spectra both with and without water presaturation were measured and used in the calculation of metabolite concentrations. Reported resonance integrals of spermine at 3.09–1.13 ppm and citrate at 2.52–2.73 ppm are integrals of curve-fittings according to Lorentzian line-shapes. The broad resonance(s) of spermine were fitted by two–four Lorentzians that could best represent the total area of the region, while four Lorentzians were used to fit each of the citrate signals at 2.52, 2.56, 2.69, and 2.73 ppm.

Tissue water signals, measured from spectra without water presaturation, were used as an internal standard for the estimation of the concentration of cellular metabolites. The concentrations of a metabolite ([M]) were calculated by using the following formula:

$$[M] = \frac{I_M/m}{I_{H_2O}/2} \cdot \frac{I_{Met/H_2O}}{I_{Met}} \cdot 80\% \cdot 55.56 \cdot 10^3 \ (\mu mol/g),$$

where I_{H_2O} and I_{Met/H_2O} represent the intensities of tissue water and the metabolite region (0.5–4.5 ppm) from spectra without water presaturation, respectively; I_M and I_{Met} represent the intensities of the metabolite of interest and the same metabolite region measured from spectra with water presaturation; and m is the number of protons of the metabolite that give rise to the resonance of I_M. The estimation is also based on the approximation that tissue contains 80% (weight) of water, i.e. 44 mmol/g. The regional metabolic intensities integrated from 0.5 to 4.5 ppm for both spectra were used to convert intensities of water and the metabolite of interest integrated separately from these two spectra measured with different experimental parameters into a comparable common scale.

2.4. Statistical analysis

Upon the completion of both NMR and histopathology measurements, the two sets of data were combined and analyzed with the statistical program JMP (SAS Institute, Cary, NC, USA). Correlations between metabolite concentrations and the vol% of normal prostatic epithelial cells were evaluated by bivariate linear least squares fits.
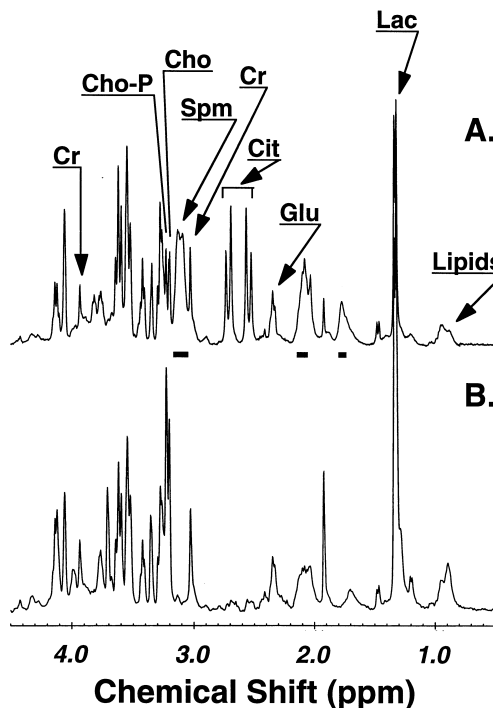

Fig. 1. 400 MHz HRMAS proton MR spectra (water-suppressed, T2-filtered) obtained from intact but previously frozen tissue: (A) normal human prostate; (B) tumor-bearing prostate.

3. Results and discussion

3.1. High resolution proton NMR spectra of intact prostate tissue specimens

Fig. 1 shows examples of HRMAS ^{1}H NMR spectra (water-suppressed, T2-filtered) obtained with the same measurement protocol from intact human tissue specimens of normal prostate (A) and prostate cancer (B). Fig. 1A presents cellular metabolites observed in a specimen containing 45 vol% of epithelial cells and 55 vol% stroma structure, as determined by histopathological quantification of the specimen after its NMR measurement. Fig. 1B profiles a specimen containing 23 vol% malignancy, 17 vol% epithelial cells and 60 vol% stroma. Labels in the figure indicate selected resonances.

Major differences between Fig. 1A and Fig. 1B are in the regions labeled as spermine (Spm) and citrate (Cit). Spermine has the symmetrical structure NH_2-$(CH_2)_3$-NH-$(CH_2)_4$-NH-$(CH_2)_3$-NH_2 with five types of methylene groups giving rise to complex multiplet signals at 3.09–3.13 ppm (-CH_2-N, 12H), 2.09–2.10 ppm (N-CH_2-CH_2-CH_2-N, 4H) and 1.78 ppm (N-CH_2-CH_2-CH_2-CH_2-N, 4H), whereby the latter two signals overlap with signals from amino acids. For this reason, only the signals for methylenes next to amino groups could be used in the analysis. These resonance regions of spermine are labeled with horizontal bars beneath Fig. 1A. At high magnetic field strength, citrate exhibits a well-resolved four-line pseudo-quartet pattern (AB spin system) for the three chemically equivalent methylene groups (6H). Normal tissue (Fig. 1A)

shows an abundance of these two metabolites, while the cancerous specimen (Fig. 1B) exhibits severe depletion in both metabolites. The signal assignments are based on both the literature [5–8] and our own measurements of authentic compounds of spermine, spermidine, and putrescine using the same experimental conditions as those used for tissue analysis (data not shown). Although other polyamines (putrescine and spermidine) would also have resonances in the 3.09–3.13 ppm region, our results confirmed that spermine is the predominant polyamine in prostate as previously reported [11–13].

3.2. Histopathology evaluation

Histopathological evaluation was then conducted on the airs of adjacent specimens taken from each case. Fig. 2 compares such a pair of specimens from a tumor-bearing prostate (with examples of cancer cells indicated by arrows). We observed a slightly compromised histopathological quality for specimens that had gone through HRMAS analysis when compared with their paired counterpart, especially when cellular details were examined at a high power of magnification. Nevertheless, the overall histopathological integrity of these specimens was sufficiently preserved to permit the quantification of adenocarcinoma cells, normal epithelial cells, and stroma structure in the specimen. Notably, among 15 clinical cases of prostate adenocarcinomas (Gleason scores: 6/10 and 7/10), cancer cells were only detected histopathologically in three cases (20%) of the surgical specimens available for this study. In other words, had we not been able to perform
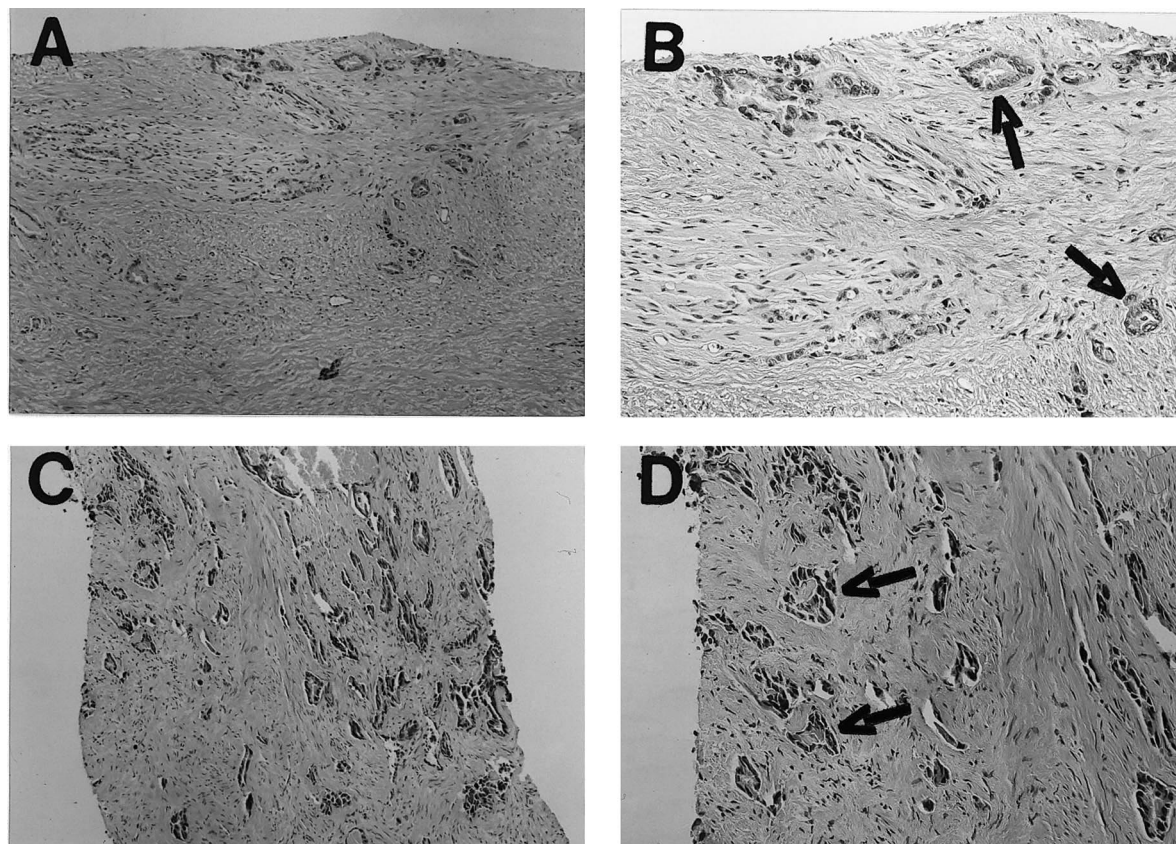

Fig. 2. Examples of histopathological images obtained from a pair of adjacent prostate tissue specimens taken from the same tumor-bearing prostate. A,B: Tissue not subjected to HRMAS NMR (50×, 100× magnification); C,D: adjacent tissue after HRMAS NMR analysis (50×, 100×).
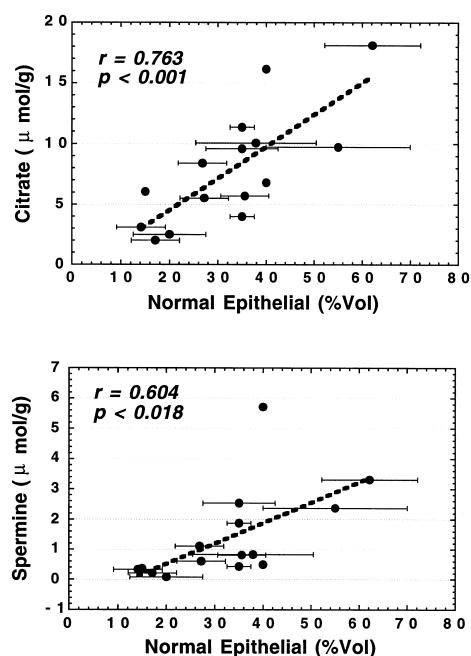
Fig. 3. Linear regression analysis for tissue concentrations of citrate (top) and spermine (bottom) vs. vol% of normal prostate epithelial cells for 15 specimens subjected to HRMAS NMR analysis and histopathology of serial sections.

histopathology after NMR evaluation, we would have had no means by which to recognize that 80% of the samples that were studied with NMR contained no cancer cells.

3.3. Quantitative correlations between spectroscopy and histopathology

Fig. 3 presents a linear regression analysis for the tissue concentration of (Fig. 3, top) citrate and (Fig. 3, bottom) spermine as a function of the vol% of normal epithelial cells, as determined for each specimen. These statistically significant correlations for citrate ($r^2 = 0.582$, $P < 0.001$) and spermine ($r^2 = 0.365$, $P < 0.018$) suggest that the two metabolites likely are either produced by or reside in the normal epithelial cells of the prostate.

We notice the proposed biological importance of spermine in relation to the growth of human prostate cancer, and recognize the potential interests that may be generated by this study. In order for us to be entirely confident in our interpretation of spermine (Fig. 3, bottom), we compared spermine with citrate, as determined by the same protocol (Fig. 3, top). Compared with spermine, citrate has been widely studied as a prostate metabolite by both in vivo and ex vivo NMR [8,14,15]. Citrate, a secretory product under androgenic control, presents in high concentrations in the prostate. Since its well-resolved typical AB spin pseudo-quartet signal pattern [13] appears in a spectral region of 2.52–2.73 ppm that is relatively free of resonances from other metabolites, both in vivo and previously published ex vivo studies had little difficulty in detecting citrate. A reduction in citrate has consistently been associated with prostate cancers measured in clinic in vivo NMR spectroscopy [14,15]. Our results indicate the 58% of the variance in tissue citrate can be assigned to the vol% of normal prostatic epithelial cells. This correlation,

which is demonstrated here for the first time by combined histological and spectroscopic analysis of individual tissue samples, provides an explanation for the well-established observation of reduction of citrate in prostate cancer [16].

Spermine in intact specimens has been more difficult to measure than citrate because, with conventional proton NMR methods for solution, sample heterogeneity frequently results in linebroadening. As a result of this, resonances at 3.1 ppm cannot be resolved from neighboring signals, including those from creatine (3.03 ppm) and choline compounds (3.20–3.30 ppm). However, HRMAS allows us to remove the residual solid-like effects, such as magnetic susceptibility, to quantify spermine in intact specimens and to relate concentration to the population of prostate epithelial cells.

It is important to note that our measurements of intact prostate tissue also resulted in a strong linear correlation between spermine and citrate ($r^2 = 0.75$, $P < 0.0001$, figures not shown), in close agreement with the observation made by Lynch and Nicholson with respect to human prostatic fluid [13]. Although further molecular studies are needed to confirm speculation about the existence of a molecular complex between the oppositely polared spermine and citrate, we nevertheless consider such a postulation to be a reasonable hypothesis that may explain the apparent ionic neutrality of the system and the reasonable chemical shift values of these metabolites [13].

Finally, we wish to note that the newly established relationships between spermine levels and normal prostatic epithelial cells may allow us to carry out further investigations on human subjects, and to explore possible relationships between the mechanism of spermine in prostatic epithelial cells and the aggression of prostate cancer as observed and documented in the clinic.

References

[1] Smith, R., Litwin, M., Lu, Y. and Zetter, B. (1995) Nat. Med. 1, 1040–1045.
[2] Degeorges, A., Tatoud, R., Fauvel-Lafeve, F., Podgorniak, M.-P., Millot, G., de Cremoux, P. and Calvo, F. (1996) Int. J. Cancer 68, 207–214.
[3] Gately, S. et al. (1996) Cancer Res. 56, 4887–4890.
[4] Mountford, C., Doran, S., Lean, C. and Russell, P. (1997) Biophys. Chem. 68, 127–135.
[5] Schiebler, M., Miyamoto, K., White, M., Maygarden, S. and Mohler, J. (1993) Magn. Reson. Med. 29, 285–291.
[6] Lynch, M., Masters, J., Pryor, J., Lindon, J., Spraul, M., Foxall, P. and Nicholson, J. (1994) J. Pharm. Biomed. Anal. 12, 5–19.
[7] Cornel, E., Smits, G., de Ruijter, J., Oosterhof, G., Heerschap, A., Debruyne, F. and Schalken, J. (1995) Prostate 26, 275–280.
[8] Hahn, P., Smith, I., Leboldus, L., Littman, C., Somorjai, R. and Bezabeh, T. (1997) Cancer Res. 57, 3398–3401.
[9] Cheng, L.L., Lean, C., Bogdanova, A., Wright, J., Ackerman, J., Brady, T. and Garrido, L. (1996) Magn. Reson. Med. 36, 653–658.
[10] Cheng, L., Anthony, D., Comite, A., Black, P., Tzika, A. and Gonzalez, R. (2000) Neuro-Oncology 2, 87–95.

[11] Willker, W., Flogel, U. and Leibfritz, D. (1998) NMR Biomed. 11, 47–54.
[12] van der Graaf, M., Schipper, R., Oosterhof, G., Schalken, J., Verhofstad, A. and Heerschap, A. (2000) MAGMA 10, 153–159.
[13] Lynch, M. and Nicholson, J. (1997) Prostate 30, 248–255.
[14] van der Graaf, M., van den Boogert, H., Jager, G., Barentsz, J. and Heerschap, A. (1999) Radiology 213, 919–925.
[15] Males, R., Vigneron, D., Star-Lack, J., Falbo, S., Nelson, S., Hricak, H. and Kurhanewicz, J. (2000) Magn. Reson. Med. 43, 17–22.
[16] Costello, L., Franklin, R. and Narayan, P. (1999) Prostate 38, 237–245.